

AS

SW 9439



SCAN-9409190

ICHEP94 Ref. GLS0740
Submitted to PA 16,2 P1 9,19

CLEO CONF 94-17
July 19, 1994

New Decay Modes of the Λ_c^+ Charm Baryon

M. Bishai,¹ J. Fast,¹ E. Gerndt,¹ R.L. McIlwain,¹ T. Miao,¹ D.H. Miller,¹ M. Modesitt,¹ D. Payne,¹ E.I. Shibata,¹ I.P.J. Shipsey,¹ P.N. Wang,¹ M. Battle,² J. Ernst,² L. Gibbons,² Y. Kwon,² S. Roberts,² E.H. Thorndike,² C.H. Wang,² J. Dominick,³ M. Lambrecht,³ S. Sanghera,³ V. Shelkov,³ T. Skwarnicki,³ R. Stroynowski,³ I. Volobouev,³ G. Wei,³ P. Zadorozhny,³ M. Artuso,⁴ M. Gao,⁴ M. Goldberg,⁴ D. He,⁴ N. Horwitz,⁴ G.C. Moneti,⁴ R. Mountain,⁴ F. Muheim,⁴ Y. Mukhin,⁴ S. Playfer,⁴ Y. Rozen,⁴ S. Stone,⁴ X. Xing,⁴ G. Zhu,⁴ J. Bartelt,⁵ S.E. Csorna,⁵ Z. Egyed,⁵ V. Jain,⁵ D. Gibaut,⁶ K. Kinoshita,⁶ P. Pomianowski,⁶ B. Barish,⁷ M. Chadha,⁷ S. Chan,⁷ D.F. Cowen,⁷ G. Eigen,⁷ J.S. Miller,⁷ C. O'Grady,⁷ J. Urheim,⁷ A.J. Weinstein,⁷ M. Athanas,⁸ W. Brower,⁸ G. Masek,⁸ H.P. Paar,⁸ M. Sivertz,⁸ J. Gronberg,⁹ R. Kutschke,⁹ S. Menary,⁹ R.J. Morrison,⁹ S. Nakanishi,⁹ H.N. Nelson,⁹ T.K. Nelson,⁹ C. Qiao,⁹ J.D. Richman,⁹ A. Ryd,⁹ H. Tajima,⁹ D. Sperka,⁹ M.S. Witherell,⁹ R. Balest,¹⁰ K. Cho,¹⁰ W.T. Ford,¹⁰ D.R. Johnson,¹⁰ K. Lingel,¹⁰ M. Lohner,¹⁰ P. Rankin,¹⁰ J.G. Smith,¹⁰ J.P. Alexander,¹¹ C. Bebek,¹¹ K. Berkelman,¹¹ K. Bloom,¹¹ T.E. Browder,^{11*} D.G. Cassel,¹¹ H.A. Cho,¹¹ D.M. Coffman,¹¹ D.S. Crowcroft,¹¹ P.S. Drell,¹¹ D. Dumas,¹¹ R. Ehrlich,¹¹ P. Gaidarev,¹¹ R.S. Galik,¹¹ M. Garcia-Sciveres,¹¹ B. Geiser,¹¹ B. Gittelman,¹¹ S.W. Gray,¹¹ D.L. Hartill,¹¹ B.K. Heltsley,¹¹ S. Henderson,¹¹ C.D. Jones,¹¹ S.L. Jones,¹¹ J. Kandaswamy,¹¹ N. Katayama,¹¹ P.C. Kim,¹¹ D.L. Kreinick,¹¹ G.S. Ludwig,¹¹ J. Masui,¹¹ J. Mevissen,¹¹ N.B. Mistry,¹¹ C.R. Ng,¹¹ E. Nordberg,¹¹ J.R. Patterson,¹¹ D. Peterson,¹¹ D. Riley,¹¹ S. Salman,¹¹ M. Sapper,¹¹ F. Würthwein,¹¹ P. Avery,¹² A. Freyberger,¹² J. Rodriguez,¹² S. Yang,¹² J. Yelton,¹² D. Cinabro,¹³ T. Liu,¹³ M. Saulnier,¹³ R. Wilson,¹³ H. Yamamoto,¹³ T. Bergfeld,¹⁴ B.I. Eisenstein,¹⁴ G. Gollin,¹⁴ B. Ong,¹⁴ M. Palmer,¹⁴ M. Selen,¹⁴ J. J. Thaler,¹⁴ K.W. Edwards,¹⁵ M. Ogg,¹⁵ A. Bellerive,¹⁶ D.I. Britton,¹⁶ E.R.F. Hyatt,¹⁶ D.B. MacFarlane,¹⁶ P.M. Patel,¹⁶ B. Spaan,¹⁶ A.J. Sadoff,¹⁷ R. Ammar,¹⁸ P. Baringer,¹⁸ A. Bean,¹⁸ D. Besson,¹⁸ D. Coppage,¹⁸ N. Coptly,¹⁸ R. Davis,¹⁸ N. Hancock,¹⁸ M. Kelly,¹⁸ S. Kotov,¹⁸ I. Kravchenko,¹⁸ N. Kwak,¹⁸ H. Lam,¹⁸ Y. Kubota,¹⁹ M. Lattery,¹⁹ M. Momayezi,¹⁹ J.K. Nelson,¹⁹ S. Patton,¹⁹ R. Poling,¹⁹ V. Savinov,¹⁹ S. Schrenk,¹⁹ R. Wang,¹⁹ M.S. Alam,²⁰ I.J. Kim,²⁰ Z. Ling,²⁰ A.H. Mahmood,²⁰ J.J. O'Neill,²⁰ H. Severini,²⁰ C.R. Sun,²⁰ F. Wappler,²⁰ G. Crawford,²¹ C. M. Daubenmier,²¹ R. Fulton,²¹ D. Fujino,²¹ K.K. Gan,²¹ K. Honscheid,²¹ H. Kagan,²¹ R. Kass,²¹ J. Lee,²¹ R. Malchow,²¹ M. Sung,²¹ C. White,²¹ M.M. Zoeller,²¹ F. Butler,²² X. Fu,²² B. Nemati,²² W.R. Ross,²² P. Skubic,²² and M. Wood²²

(CLEO Collaboration)

- ¹Purdue University, West Lafayette, Indiana 47907
²University of Rochester, Rochester, New York 14627
³Southern Methodist University, Dallas, Texas 75275
⁴Syracuse University, Syracuse, New York 13244
⁵Vanderbilt University, Nashville, Tennessee 37235
⁶Virginia Polytechnic Institute and State University, Blacksburg, Virginia, 24061
⁷California Institute of Technology, Pasadena, California 91125
⁸University of California, San Diego, La Jolla, California 92093
⁹University of California, Santa Barbara, California 93106
¹⁰University of Colorado, Boulder, Colorado 80309-0390
¹¹Cornell University, Ithaca, New York 14853
¹²University of Florida, Gainesville, Florida 32611
¹³Harvard University, Cambridge, Massachusetts 02138
¹⁴University of Illinois, Champaign-Urbana, Illinois, 61801
¹⁵Carleton University, Ottawa, Ontario K1S 5B6 and the Institute of Particle Physics, Canada
¹⁶McGill University, Montréal, Québec H3A 2T8 and the Institute of Particle Physics, Canada
¹⁷Ithaca College, Ithaca, New York 14850
¹⁸University of Kansas, Lawrence, Kansas 66045
¹⁹University of Minnesota, Minneapolis, Minnesota 55455
²⁰State University of New York at Albany, Albany, New York 12222
²¹Ohio State University, Columbus, Ohio, 43210
²²University of Oklahoma, Norman, Oklahoma 73019

Abstract

We have observed four new decay modes of the charmed baryon Λ_c^+ using data collected with the CLEO II detector. Three decay modes, $\Lambda_c^+ \rightarrow p\bar{K}^0\eta$, $\Lambda\eta\pi^+$, and $\Sigma^+\eta$, are first observations of final states with an η meson, while the fourth mode, $\Lambda_c^+ \rightarrow \Lambda\bar{K}^0K^+$, requires an $s\bar{s}$ quark pair to be popped out of the vacuum. The branching ratios relative to $\Lambda_c^+ \rightarrow pK^-\pi^+$ are measured to be $0.25 \pm 0.05 \pm 0.04$, $0.36 \pm 0.06 \pm 0.05$, $0.10 \pm 0.03 \pm 0.02$, and $0.11 \pm 0.02 \pm 0.02$, respectively.

*Permanent address: University of Hawaii at Manoa

I. INTRODUCTION

In the past year, CLEO has measured the exclusive decays of the Λ_c^+ into $\Lambda(n\pi)^+$, $\Sigma^0(n\pi)^+$, $\Sigma^+(n\pi)^0$, $pK^-(n\pi)^+$, and $pK_s^0(n\pi)^0$, where $n \leq 3$ and includes up to one π^0 [1–4]. In addition, CLEO has observed decays that are expected to occur solely through the W-exchange diagram, namely, $\Lambda_c^+ \rightarrow \Sigma^+K^+K^-$, Ξ^0K^+ , and $\Xi^-K^+\pi^+$ [5]. Figure 1 displays these branching fractions relative to the normalizing decay mode $\Lambda_c^+ \rightarrow pK^-\pi^+$. Many of these modes were first observations, especially modes that contain neutral particles, for which the CLEO detector is highly efficient. Using the PDG value of $\mathcal{B}(\Lambda_c^+ \rightarrow pK^-\pi^+) = (3.2 \pm 0.7)\%$ [6], only $\sim 25\%$ of the Λ_c^+ hadronic decay modes have been observed. Missing from this catalog of Λ_c^+ decays are higher multiplicity modes, especially those that have multiple π^0 's. Also missing are decay modes that have Σ^- hyperons or neutrons in the final state since these decays are difficult to observe. There are clearly a substantial number of Λ_c^+ decay modes which remain to be discovered.

This paper presents new results on four Λ_c^+ decay modes. These include the first observation of three Λ_c^+ decay modes with η 's in the final state, namely $\Lambda_c^+ \rightarrow pK_s^0\eta$, $\Lambda\eta\pi^+$, and $\Sigma^+\eta$. The fourth mode is $\Lambda_c^+ \rightarrow \Lambda K_s^0K^+$, which involves popping an $s\bar{s}$ quark pair.

II. PARTICLE IDENTIFICATION

The data were collected with the CLEO II detector at the Cornell e^+e^- storage ring CESR, which operated on, and just below, the $\Upsilon(4S)$ resonance. The CLEO II detector [7] is a large solenoidal detector with 67 tracking layers and a CsI electromagnetic calorimeter that provides efficient π^0 and η reconstruction. We have used a total integrated luminosity of 3.25 fb^{-1} , which corresponds to roughly 4 million $c\bar{c}$ events.

Most of the Λ_c^+ decay modes discussed in this report have an η meson in the final state. The η candidates are selected through their decay $\eta \rightarrow \gamma\gamma$ from pairs of well-defined showers in the CsI calorimeter. To reduce combinatorics from soft photons, we require $E_\gamma > 0.15 \text{ GeV}$ for each photon candidate and $P_\eta > 0.5 \text{ GeV}/c$. The photon candidates must not be associated with charged tracks and must have lateral shower shapes consistent with that expected for true photons [8]. At least one of the photon candidates must lie in the good barrel region ($|\cos\theta| < 0.71$). Finally, photons are vetoed if they can be paired with a second photon such that the $\gamma\gamma$ pair has an invariant mass within 2.5σ of the π^0 mass and a momentum greater than $1.0 \text{ GeV}/c$. From Monte Carlo simulations, the efficiency for detecting η 's with $P_\eta > 0.5 \text{ GeV}/c$ is about 30%. Figure 2 shows the $M_{\gamma\gamma}$ distribution after all the cuts have been applied. The η signal has a width of approximately $14 \text{ MeV}/c^2$ and a mean consistent with the true η mass. Since the signal shape is asymmetric, we select η candidates in the mass range $M_{\gamma\gamma} = 515 - 575 \text{ MeV}/c^2$. Finally, we kinematically fit the photon momenta to the nominal η mass in order to improve the η momentum estimate.

Protons, kaons, and pions are identified using dE/dx and time-of-flight information, when available. For protons we require $\text{PRLEV} > 0.1$, where PRLEV is the relative probability that the track is a proton

$$\text{PRLEV} = \frac{\mathcal{P}(p)}{\mathcal{P}(p) + \mathcal{P}(K) + \mathcal{P}(\pi)} \quad (1)$$

and \mathcal{P} is the χ^2 probability that the track satisfies a given hypothesis. Strong proton identification ($\text{PRLEV} > 0.9$) is employed for modes with high background levels, *e.g.* $\Lambda_c^+ \rightarrow pK_s^0\eta$. A track is considered as a kaon candidate if the probability $\mathcal{P}(K)$ is at least 1%. Finally, we require that a track have a dE/dx measurement consistent with the pion hypothesis (within $\pm 3\sigma$) to be identified as a pion. We use a pure sample of $\Lambda \rightarrow p\pi^-$, $D^0 \rightarrow K^-\pi^+$ from D^{*+} 's, and $K_s^0 \rightarrow \pi^+\pi^-$ to measure the particle identification efficiency for protons, kaons, and pions, respectively. The efficiency for weak and strong proton identification as a function of proton momentum is shown in Figure 3. Weak proton identification is 95% efficient for momenta below $0.5 \text{ GeV}/c$ and falls smoothly to 85% at $2.5 \text{ GeV}/c$. Strong proton identification improves the signal to noise, but quickly becomes inefficient above $1.5 \text{ GeV}/c$. Charged pions and kaons are identified with an efficiency of $\sim 99\%$ and $\sim 96\%$, respectively.

K_s^0 and Λ candidates are selected through their decays $K_s^0 \rightarrow \pi^+\pi^-$ and $\Lambda \rightarrow p\pi^-$ by reconstructing a secondary decay vertex. Detached vertices are reconstructed from the intersection of two oppositely charged tracks in the $r - \phi$ plane. We cut on the impact parameter of the daughter tracks, and require that the decay length be at least 1 mm from the interaction point in the $r - \phi$ plane. We also cut on the χ^2 of the reconstructed decay vertex, which requires both the miss distance in \hat{z} between the two tracks at the estimated decay vertex and the impact parameter of the K_s^0 or Λ to be small. The proton for the Λ candidate must satisfy $\text{PRLEV} > 0.1$. Finally, the invariant masses of the K_s^0 and Λ candidates must be within $15 \text{ MeV}/c^2$ and $5 \text{ MeV}/c^2$ of their nominal values, respectively.

The Σ^+ particle is identified through its decay into $p\pi^0$ [3]. The Σ^+ lifetime is long ($c\tau = 2.4 \text{ cm}$), hence protons from Σ^+ decays have large impact parameters. The proton candidate must have an impact parameter greater than 0.6 mm, a momentum greater than $0.5 \text{ GeV}/c$, and $\text{PRLEV} > 0.1$. The π^0 candidate is chosen from pairs of shower clusters not matched to charged tracks. The photons must have $E_\gamma > 30 \text{ MeV}$ and a lateral shower shape consistent with that of a true photon. At least one of the photons must lie in the good barrel region, and $P_{p\pi^0}$ must be greater than $0.2 \text{ GeV}/c$. The π^0 and Σ^+ invariant masses are initially computed assuming the particles originate from the primary vertex. These mass measurements are refined by recomputing them at the location of the Σ^+ decay vertex. The procedure is as follows: the Σ^+ candidate is assumed to originate from the primary vertex. We then estimate the Σ^+ decay vertex to be the point along the proton trajectory where the proton and Σ^+ intersect in the $r - \phi$ plane. We require that the miss distance between the proton and the Σ^+ along the beam axis (\hat{z}) be less than 10 mm, the recomputed π^0 mass be $120 - 150 \text{ MeV}/c^2$, and the decay vertex lie in the direction of the Σ^+ momentum. The $M_{p\pi^0}$ spectrum for $P_{p\pi^0} > 1 \text{ GeV}/c$ is shown in Figure 4. We observe $13100 \pm 300 \Sigma^+$ hyperons with a width of $5.0 \pm 0.1 \text{ MeV}/c^2$ and a mass of $1188.8 \pm 0.1 \text{ MeV}/c^2$, consistent with the nominal Σ^+ mass. Without the vertex correction, the $M_{p\pi^0}$ signal would be considerably broader. The efficiency for reconstructing $\Sigma^+ \rightarrow p\pi^0$ decays in this momentum range is about 15%. We select Σ^+ candidates that lie within $15 \text{ MeV}/c^2$ of the nominal Σ^+ mass.

Finally, charged tracks that do not arise from long-lived particles (Λ , K_s^0 , and Σ^+) must have a distance of closest approach in the $r - \phi$ plane of less than 5 mm to the interaction point, and be within 5 cm in \hat{z} .

III. $\Lambda_c^+ \rightarrow pK_s^0\eta$

The decay mode $\Lambda_c^+ \rightarrow pK_s^0\eta$ may occur via an internal spectator diagram or a W-exchange diagram; the external spectator diagram cannot contribute. The selection of protons, K_s^0 's, and η 's has been described in the previous section. Charm baryons from e^+e^- interactions are produced with a hard momentum spectrum, so we can reduce the combinatoric background by requiring $x_p(\Lambda_c^+) > 0.5$, where $x_p(\Lambda_c^+) = P_{\Lambda_c^+} / \sqrt{E_{beam}^2 - M_{\Lambda_c^+}^2}$ is the scaled momentum of the Λ_c^+ . The x_p cut also eliminates Λ_c^+ baryons that arise from B meson decays. We further require that the Fox-Wolfram event shape parameter R_2 [9] be greater than 0.2, so that the background contribution in the Λ_c^+ signal region due to $B\bar{B}$ production is reduced. The R_2 cut is used for all Λ_c^+ decay modes.

In addition, we impose strong particle ID on the proton, and require the three daughter particles to be in the same jet hemisphere by demanding that the daughter tracks lie within 90 degrees of the Λ_c^+ momentum vector. The invariant mass distribution for $\Lambda_c^+ \rightarrow pK_s^0\eta$ in the data is shown in Figure 5. We fit the signal to a Gaussian and the background to a 3rd order Chebyshev polynomial. The Gaussian width is fixed to the Monte Carlo prediction of 6.6 MeV/ c^2 , while the mean is allowed to float. We observe 53 ± 10 $pK_s^0\eta$ events at a mass of 2287 ± 2 MeV/ c^2 (statistical error only), consistent with the nominal Λ_c^+ mass. Backgrounds from misidentified D^+ and D_s^+ decays to $K_s^0\eta\pi^+$ in which the pion has been misidentified as a proton are not observed.

Since we do not know the overall Λ_c^+ cross section, we convert our observation into a branching fraction relative to the well measured decay $\Lambda_c^+ \rightarrow pK^-\pi^+$. We apply the same proton identification (PRLEV > 0.9) and Λ_c^+ momentum cut ($x_p > 0.5$) to the $\Lambda_c^+ \rightarrow pK^-\pi^+$ sample in order to reduce the systematic errors associated with these cuts. In addition, the daughter tracks are required to lie in the same jet hemisphere. A fit to the $pK^-\pi^+$ invariant mass distribution using the Monte Carlo predicted width yields 4910 ± 134 events. For $x_p > 0.5$ the Monte Carlo-based efficiencies to reconstruct the decay modes $\Lambda_c^+ \rightarrow pK_s^0\eta$ and $\Lambda_c^+ \rightarrow pK^-\pi^+$ are $(7.3 \pm 0.2)\%$ and $(22.3 \pm 0.3)\%$, respectively. After taking into account the \bar{K}^0 and η branching fractions to the final states we observe them in, the ratio of branching fractions is

$$\frac{\mathcal{B}(\Lambda_c^+ \rightarrow p\bar{K}^0\eta)}{\mathcal{B}(\Lambda_c^+ \rightarrow pK^-\pi^+)} = 0.25 \pm 0.05 \pm 0.04 \quad (2)$$

where the first error is statistical and the second is systematic (to be discussed later). This decay rate is about 2.5 times smaller than the related mode in which the η is replaced by a π^0 , which CLEO [4] measures to be $\mathcal{B}(\Lambda_c^+ \rightarrow p\bar{K}^0\pi^0)/\mathcal{B}(\Lambda_c^+ \rightarrow pK^-\pi^+) = 0.63 \pm 0.13$. This is consistent with the light quark content of the η being roughly one-third that of the π^0 .

IV. $\Lambda_c^+ \rightarrow \Lambda\eta\pi^+$

The decay $\Lambda_c^+ \rightarrow \Lambda\eta\pi^+$ can occur through three diagrams: external spectator, internal spectator and W-exchange. To reduce the combinatoric background, we require the Λ , π^+ , and η to be in the same jet hemisphere. We also place a higher momentum cut on the Λ_c^+ , namely $x_p > 0.6$, as the backgrounds are higher in this decay mode. The invariant

mass distribution for $\Lambda\eta\pi^+$ is shown in Figure 6. The signal is fit to a Gaussian with the width fixed to the Monte Carlo expectation of $\sigma_{\Lambda_c^+} = 8.6$ MeV/ c^2 , and the background is parametrized by a 2nd order Chebyshev polynomial. We observe 109 ± 16 events at a mass of 2289 ± 2 MeV/ c^2 .

Because we impose only weak particle ID on the proton, about 3% of the Λ candidates are actually K_s^0 particles. Backgrounds may arise from D^+ and D_s^+ decays to $K_s^0\eta\pi^+$, where the K_s^0 has been misidentified as a Λ . Examination of the $K_s^0\eta\pi^+$ and K_s^0 invariant mass spectra for combinations passing the selection criteria show no evidence for such backgrounds.

Applying the same proton identification and x_p cut to the $pK^-\pi^+$ sample yields 6282 ± 243 events. For $x_p > 0.6$ the efficiency to reconstruct the $\Lambda_c^+ \rightarrow \Lambda\eta\pi^+$ and $\Lambda_c^+ \rightarrow pK^-\pi^+$ decays modes are $(8.5 \pm 0.3)\%$ and $(44.2 \pm 0.5)\%$, respectively. The $pK^-\pi^+$ efficiency is higher here than in the previous case due to the looser proton identification requirement. After accounting for the Λ and η branching fractions, the ratio of branching fractions is

$$\frac{\mathcal{B}(\Lambda_c^+ \rightarrow \Lambda\eta\pi^+)}{\mathcal{B}(\Lambda_c^+ \rightarrow pK^-\pi^+)} = 0.36 \pm 0.06 \pm 0.05 \quad (3)$$

This again is about a factor of two smaller than the related decay mode $\Lambda_c^+ \rightarrow \Lambda\pi^+\pi^0$ in which the η has been replaced by a π^0 . For this mode, CLEO [2] has measured $\mathcal{B}(\Lambda_c^+ \rightarrow \Lambda\pi^+\pi^0)/\mathcal{B}(\Lambda_c^+ \rightarrow pK^-\pi^+) = 0.73 \pm 0.09 \pm 0.16$.

We have also studied the resonant substructure for the decay $\Lambda_c^+ \rightarrow \Lambda\eta\pi^+$. In addition to non-resonant phase space decays, two decay chains are possible: $\Lambda_c^+ \rightarrow \Sigma^+(1385)\eta$ with $\Sigma^+(1385) \rightarrow \Lambda\pi^+$, and $\Lambda_c^+ \rightarrow \Lambda a_0^+(980)$ with $a_0^+(980) \rightarrow \eta\pi^+$. Figure 7 shows the Dalitz plot of $M_{\Lambda\pi^+}^2$ versus $M_{\eta\pi^+}^2$ for $\Lambda\eta\pi^+$ candidates within $\pm 2\sigma$ of the Λ_c^+ mass. In order to increase the Λ_c^+ signal-to-background ratio, we have tightened the π^0 veto for η candidates by eliminating photons that are consistent with arising from a π^0 of any momentum. Both the $\Sigma^+(1385)$ and $a_0^+(980)$ are broad resonances [10]. Evidence for $\Sigma^+(1385)$ would appear as a band at $M_{\Lambda\pi^+}^2 \approx 1.9$ (GeV/ c^2) 2 . Similarly, a band at $M_{\eta\pi^+}^2 \approx 0.96$ (GeV/ c^2) 2 would indicate presence of the scalar $a_0(980)$ resonance. In Figure 8(a) we have projected the Dalitz plot onto the $M_{\Lambda\pi^+}^2$ axis and performed a Λ_c^+ sideband subtraction. A fit to the $M_{\Lambda\pi^+}^2$ distributions using the Monte Carlo distributions for $M_{\Lambda\pi^+}^2$ from $\Sigma^+(1385)\eta$ resonant and phase space decays suggests that $(37 \pm 14)\%$ (statistical errors only) of the $\Lambda\eta\pi^+$ signal proceeds via the $\Sigma^+(1385)$ resonance. Here, we have assumed that the different amplitudes due to resonant substructure add incoherently. Likewise, a projection onto the $M_{\eta\pi^+}^2$ axis suggests that $(39 \pm 14)\%$ of the $\Lambda\eta\pi^+$ signal proceeds through the $a_0(980)$ resonance, seen in Figure 8(b). However, an upper limit of 33% (90% CL) can also be placed on this process because no significant $a_0^+(980) \rightarrow K_s^0K^+$ resonant substructure is evident in the related decay mode $\Lambda_c^+ \rightarrow \Lambda K_s^0K^+$, as is discussed in Section VI. Here, we have assumed that $\mathcal{B}(a_0(980) \rightarrow \bar{K}^0K^+)/\mathcal{B}(a_0(980) \rightarrow \eta\pi^+) = 0.25 \pm 0.05$ [11].

V. $\Lambda_c^+ \rightarrow \Sigma^+\eta$

The two-body decay $\Lambda_c^+ \rightarrow \Sigma^+\eta$ is particularly significant since this decay is not expected to arise via an external spectator diagram. Identification of the Σ^+ and η candidates is described in Section II. Because four photons exist in the final state, the combinatoric

TABLE I. Comparison of experimental branching fractions to theoretical predictions for the two-body decays $\Lambda_c^+ \rightarrow \Sigma^+\pi^0$ and $\Sigma^+\eta$ relative to $\mathcal{B}(\Lambda_c^+ \rightarrow pK^-\pi^+)$.

| | $\mathcal{B}(\Lambda_c^+ \rightarrow \Sigma^+\pi^0)/\mathcal{B}(pK^-\pi^+)$ | $\mathcal{B}(\Lambda_c^+ \rightarrow \Sigma^+\eta)/\mathcal{B}(pK^-\pi^+)$ |
|------------------------|---|--|
| CLEO | $0.20 \pm 0.03 \pm 0.03$ | $0.10 \pm 0.03 \pm 0.02$ |
| Körner and Krämer [12] | 0.10 | 0.05 |
| Zenczykowski [13] | 0.13 | 0.08 |

background can be severe. Photons from the π^0 tend to be extremely soft, and so the inclusion of random soft photons can still produce π^0 , Σ^+ , and Λ_c^+ candidates with invariant masses satisfying the selection criteria. As described in the particle ID section for Σ^+ , we reduce the combinatoric background by requiring the π^0 to have a momentum $P_{\pi^0} > 0.2$ GeV/c. We also demand that the η , Σ^+ , and $\Sigma^+\eta$ candidates have high momenta: $P_\eta > 0.8$ GeV/c, $P_{\Sigma^+} > 1.0$ GeV/c, and $x_p(\Lambda_c^+) > 0.6$, respectively. Figure 9 shows the $\Sigma^+\eta$ invariant mass distribution after applying all the selection cuts. We fit this distribution to a Gaussian whose width is fixed to the Monte Carlo prediction of $\sigma_{\Lambda_c^+} = 20$ MeV/c², and a quadratic background. We observe preliminary evidence for $\Lambda_c^+ \rightarrow \Sigma^+\eta$ consisting of 16.6 ± 5.2 events at a mass of 2285 ± 5 MeV/c².

Due to the soft photon background, about 12% of the time events in the data are multiply counted in the $\Sigma^+\eta$ mass distribution. The multiple entries are distributed uniformly over the mass range 2.0–2.6 GeV/c². The Monte Carlo models this effect well, and so we increase the statistical error from the fit by 6%.

Applying the same proton identification and x_p requirement on the $pK^-\pi^+$ sample yields 6282 ± 243 events. For $x_p > 0.6$ the efficiency to reconstruct the $\Lambda_c^+ \rightarrow \Sigma^+\eta$ and $\Lambda_c^+ \rightarrow pK^-\pi^+$ modes are $(5.2 \pm 0.2)\%$ and $(44.2 \pm 0.5)\%$, respectively. Accounting for the branching fractions of Σ^+ and η , we obtain the ratio of branching fractions to be

$$\frac{\mathcal{B}(\Lambda_c^+ \rightarrow \Sigma^+\eta)}{\mathcal{B}(\Lambda_c^+ \rightarrow pK^-\pi^+)} = 0.10 \pm 0.03 \pm 0.02 \quad (4)$$

This decay rate is about half that of the related two-body decay mode, $\Lambda_c^+ \rightarrow \Sigma^+\pi^0$, which has been measured by CLEO [3] to be $\mathcal{B}(\Lambda_c^+ \rightarrow \Sigma^+\pi^0)/\mathcal{B}(\Lambda_c^+ \rightarrow pK^-\pi^+) = 0.20 \pm 0.03 \pm 0.03$.

Körner and Krämer [12] and Zenczykowski [13] have made theoretical predictions for Λ_c^+ decays into two-body final states with Σ^+ hyperons. We have converted their decay rates into relative branching fractions using the PDG values for the Λ_c^+ lifetime and $\mathcal{B}(\Lambda_c^+ \rightarrow pK^-\pi^+)$ [6]. The theoretical estimates, shown in Table I, agree with our results within a factor of two. Moreover, both groups predict that the ratio $\mathcal{B}(\Sigma^+\eta)/\mathcal{B}(\Sigma^+\pi^0)$ is 0.5–0.6, in agreement with our measurement.

VI. $\Lambda_c^+ \rightarrow \Lambda K_s^0 K^+$

The decay $\Lambda_c^+ \rightarrow \Lambda K_s^0 K^+$ is analogous to the decay $\Lambda_c^+ \rightarrow \Lambda \pi^+\pi^0$ except that an $s\bar{s}$ quark pair must be popped out of the vacuum. We extract this decay mode by finding the Λ , K_s^0 ,

TABLE II. Summary of results on new Λ_c^+ decay modes. The efficiencies do not include branching fractions to the observed final states.

| Λ_c^+ decay mode | Number of events | x_p cut | Efficiency (%) | $\mathcal{B}/\mathcal{B}(\Lambda_c^+ \rightarrow pK^-\pi^+)$ |
|--------------------------|------------------|-----------|----------------|--|
| $p\bar{K}^0\eta$ | 53 ± 10 | 0.5 | 7.3 | $0.25 \pm 0.05 \pm 0.04$ |
| $\Lambda\eta\pi^+$ | 109 ± 16 | 0.6 | 8.5 | $0.36 \pm 0.06 \pm 0.05$ |
| $\Sigma^+\eta$ | 25 ± 7 | 0.6 | 5.2 | $0.10 \pm 0.03 \pm 0.02$ |
| $\Lambda\bar{K}^0K^+$ | 46 ± 8 | 0.4 | 7.9 | $0.11 \pm 0.02 \pm 0.02$ |

and K^+ as described in Section II, and by requiring the three particles to be in the same jet hemisphere. Since the phase space for this decay is small and the K_s^0 and Λ signals are relatively clean, we can relax the Λ_c^+ momentum cut to $x_p > 0.4$ without greatly increasing the combinatoric background. Figure 10 shows the $\Lambda K_s^0 K^+$ invariant mass distribution for the data, where we observe a Λ_c^+ signal of 46 ± 8 events at a mass of $M_{\Lambda_c^+} = 2286 \pm 1$ MeV/c². Here, we have fixed the Gaussian width to the Monte Carlo expectation $\sigma_{\Lambda_c^+} = 4.1$ MeV/c² and assumed a linear background.

We have checked that the decay $D^+ \rightarrow K_s^0 K_s^0 K^+$ in which a K_s^0 is misidentified as a Λ , or the doubly misidentified decay $D_s^+ \rightarrow K_s^0 K_s^0 \pi^+$ does not contribute to the Λ_c^+ signal region. We also do not observe any resonant substructure in the decay $\Lambda_c^+ \rightarrow \Lambda K_s^0 K^+$. In particular, the fraction of $K_s^0 K^+$ from the $a_0(980)$ resonance is less than 30% at the 90% confidence level.

The $\Lambda_c^+ \rightarrow pK^-\pi^+$ sample yields 9288 ± 314 events, after applying the same proton and kaon identification and x_p cut. For $x_p > 0.4$ the efficiency to reconstruct the $\Lambda_c^+ \rightarrow \Lambda K_s^0 K^+$ and $\Lambda_c^+ \rightarrow pK^-\pi^+$ decay modes are $(7.9 \pm 0.2)\%$ and $(38.1 \pm 0.4)\%$, respectively. After accounting for the Λ and \bar{K}^0 branching fractions, we obtain the ratio of branching fractions to be

$$\frac{\mathcal{B}(\Lambda_c^+ \rightarrow \Lambda\bar{K}^0K^+)}{\mathcal{B}(\Lambda_c^+ \rightarrow pK^-\pi^+)} = 0.11 \pm 0.02 \pm 0.02 \quad (5)$$

This is roughly 7 times smaller than the related decay mode without $s\bar{s}$ popping, $\Lambda_c^+ \rightarrow \Lambda\pi^+\pi^0$, which CLEO [2] measures to be $\mathcal{B}(\Lambda_c^+ \rightarrow \Lambda\pi^+\pi^0)/\mathcal{B}(\Lambda_c^+ \rightarrow pK^-\pi^+) = 0.73 \pm 0.09 \pm 0.16$. A summary of all the Λ_c^+ decay modes studied in this analysis is presented in Table II.

VII. SYSTEMATICS

The systematic errors associated with the measured branching fractions of the new Λ_c^+ decay modes are listed in Table III. The systematic errors due to uncertainties in the proton identification and the Λ_c^+ momentum spectrum are greatly reduced by normalizing the branching fraction to the reference decay mode $\Lambda_c^+ \rightarrow pK^-\pi^+$. Weak proton ID has a relatively flat efficiency over the entire proton momentum range, so uncertainties in the absolute efficiency cancel in the ratio. We are more sensitive to systematic uncertainties when tagging protons using strong particle ID since the efficiency falls off rapidly beyond

TABLE III. Sources of systematic errors.

| Source | Fractional Error (%) | | | |
|--|----------------------|--------------------|----------------|-------------------------|
| | $p\bar{K}_s^0\eta$ | $\Lambda\eta\pi^+$ | $\Sigma^+\eta$ | $\Lambda\bar{K}_s^0K^+$ |
| K_s^0 , Λ , and Σ^+ finding | 10 | 10 | 10 | 14 |
| η and π^0 finding | 5 | 5 | 7 | — |
| Tracking efficiency | — | — | 4 | 4 |
| Proton and kaon identification | 8 | 2 | 2 | — |
| $pK^-\pi^+$ substructure | 7 | 2 | 2 | 5 |
| Λ_c^+ substructure | — | 6 | — | — |
| Uncertainties in $\sigma_{\Lambda_c^+}$ | 5 | 5 | 5 | 5 |
| Monte Carlo statistics | 3 | 3 | 3 | 3 |
| TOTAL | 16 | 14 | 14 | 16 |

 TABLE IV. Comparison of relative Λ_c^+ branching fractions computed from high and low x_p regions. The errors are statistical only.

| x_p range | $B(p\bar{K}_s^0\eta)/B(pK^-\pi^+)$ | $B(\Lambda\eta\pi^+)/B(pK^-\pi^+)$ | $B(\Lambda\bar{K}_s^0K^+)/B(pK^-\pi^+)$ |
|-------------|------------------------------------|------------------------------------|---|
| 0.5-0.7 | 0.24 ± 0.06 | 0.33 ± 0.07 | 0.13 ± 0.03 |
| 0.7-1.0 | 0.28 ± 0.08 | 0.41 ± 0.07 | 0.07 ± 0.03 |

1.5 GeV/c and because the proton momentum spectrum differs between $p\bar{K}_s^0\eta$ and $pK^-\pi^+$. We vary the position of the falloff by 50 MeV/c and see a 5% difference. In addition, the efficiency-corrected $\Lambda_c^+ \rightarrow pK^-\pi^+$ yields using weak and strong proton identification differ by 8%. We take this value as the total systematic error for applying strong proton ID.

The uncertainty in modeling the Λ_c^+ momentum spectrum can cause a systematic error in the ratio of branching fractions if the Λ_c^+ reconstruction efficiency differs as a function of Λ_c^+ momentum between the two decay modes. We have measured the x_p distribution from our large sample of $\Lambda_c^+ \rightarrow pK^-\pi^+$ events and used this distribution to compute the average efficiency for each decay mode over the Λ_c^+ momentum range of interest. We assign this a systematic error of 1%. As a check, we divide the data into a high and low x_p region and compute the relative branching fraction separately for both regions, as shown in Table IV. The relative branching fractions for $p\bar{K}_s^0\eta$ and $\Lambda\eta\pi^+$ are consistent, whereas the two for $\Lambda\bar{K}_s^0K^+$ differ by 1.6σ .

We assign a systematic error of 2% for every charged track and 5% for every π^0 and η in the final state. If we require that both photons from the η come from the good barrel region, the efficiency for reconstructing $p\bar{K}_s^0\eta$ and $\Lambda\eta\pi^+$ is reduced by 30%, but the difference in the efficiency-corrected yields are within errors. The systematic error for reconstructing K_s^0 and Λ particles is studied by comparing the yields from the detached vertex reconstruction to the yields from the $\pi^+\pi^-$ and $p\pi^-$ invariant mass distributions where the masses are computed assuming the decay occurs at the origin. We perform this as a function of the K_s^0 and Λ momentum. The Monte Carlo agrees with the data to within 10%. We calculated a

10% systematic error for reconstructing Σ^+ hyperons due to the cut on the proton impact parameter and by comparing the Σ^+ yields with and without using the estimated decay vertex.

The $\Lambda_c^+ \rightarrow pK^-\pi^+$ reconstruction efficiency is sensitive to whether the Λ_c^+ decays via phase space, pK^{*0} , or $\Delta^{++}K^-$. The variation depends on the selection criteria (2-7%) and is taken as a systematic error. Also, the efficiency for reconstructing $\Lambda_c^+ \rightarrow \Lambda\eta\pi^+$ depends on whether the decay proceeds according to phase space, $\Sigma^+(1385)\eta$, or $\Sigma^+a_0(980)$. We assign a 6% systematic error due to the possible $\Lambda\eta\pi^+$ resonant substructure.

VIII. CONCLUSIONS

We have observed four new decay modes of the charmed baryon Λ_c^+ . Three decay modes, $\Lambda_c^+ \rightarrow p\bar{K}_s^0\eta$, $\Lambda\eta\pi^+$, and $\Sigma^+\eta$, contain an η particle in the final state, while the fourth decay mode, $\Lambda_c^+ \rightarrow \Lambda\bar{K}_s^0K^+$, requires an $s\bar{s}$ quark pair to pop out of the vacuum. The branching fractions relative to the reference mode $\Lambda_c^+ \rightarrow pK^-\pi^+$ are measured to be $0.25 \pm 0.05 \pm 0.04$, $0.36 \pm 0.06 \pm 0.05$, $0.10 \pm 0.03 \pm 0.02$, and $0.11 \pm 0.02 \pm 0.02$, respectively. Altogether, the new modes account for roughly 3% of all Λ_c^+ decays. The $\Lambda\eta\pi^+$ decay mode appears to have a resonant substructure via $\Sigma^+(1385)\eta$, but might also proceed through $\Sigma^+a_0(980)$.

ACKNOWLEDGEMENTS

We gratefully acknowledge the effort of the CESR staff in providing us with excellent luminosity and running conditions. This work was supported by the National Science Foundation, the U.S. Dept. of Energy, the Heisenberg Foundation, the SSC Fellowship program of TNRLC, Natural Sciences and Engineering Research Council of Canada, and the A.P. Sloan Foundation.

REFERENCES

- [1] Unless otherwise stated, the charge conjugate mode is always implied.
- [2] CLEO Collaboration, P. Avery *et al.*, Phys. Lett. B **325**, 257(1994). No significant $\Lambda\rho^+$ or $\Sigma^*(1385)\pi$ resonant substructure was evident in the $\Lambda_c^+ \rightarrow \Lambda\pi^+\pi^0$ decay mode.
- [3] CLEO Collaboration, Y. Kubota *et al.*, Phys. Rev. Lett. **71**, 3255(1993).
- [4] CLEO Collaboration, D. Cinabro *et al.*, CLEO Conf 93-27, contrib. paper in Lepton Photon Conf. (1993).
- [5] CLEO Collaboration, P. Avery *et al.*, Phys. Rev. Lett. **71**, 2391(1993).
- [6] Particle Data Group, K. Hikasa *et al.*, Phys. Rev. D **45**, 1(1992).
- [7] CLEO Collaboration, Y. Kubota *et al.*, Nucl. Inst. and Meth. **A320**, 66(1992).
- [8] The shower shape is measured by the ratio of energy in the 9 crystals nearest the shower center to the energy in the 25 crystals nearest the shower center. For photons in our detector, this ratio peaks above 0.9.
- [9] G.C. Fox and S. Wolfram, Phys. Rev. Lett. **41**, 1581(1978).
- [10] The $\Sigma^*(1385)$ full width is $\Gamma = 36 \pm 1$ MeV/ c^2 and the $a_0(980)$ full width is $\Gamma = 57 \pm 11$ MeV/ c^2 .
- [11] The PDG reports that $B(f_1(1285) \rightarrow \eta\pi\pi) = (50 \pm 5)\%$ and $B(f_1(1285) \rightarrow K\bar{K}\pi) = (11.9 \pm 1.4)\%$. The WA76 Collaboration reports that both decays are dominated by $a_0(980)\pi$ with $a_0(980) \rightarrow \eta\pi$ and $K\bar{K}$. T.A. Armstrong *et al.*, Z. Phys. C **52**, 389(1991). T.A. Armstrong *et al.*, Phys. Lett. B **221**, 216(1989).
- [12] J.G. Körner and M. Krämer, Z. Phys. C **55**, 659(1992).
- [13] P. Zenczykowski, Phys. Rev. D **50**, 402(1994).

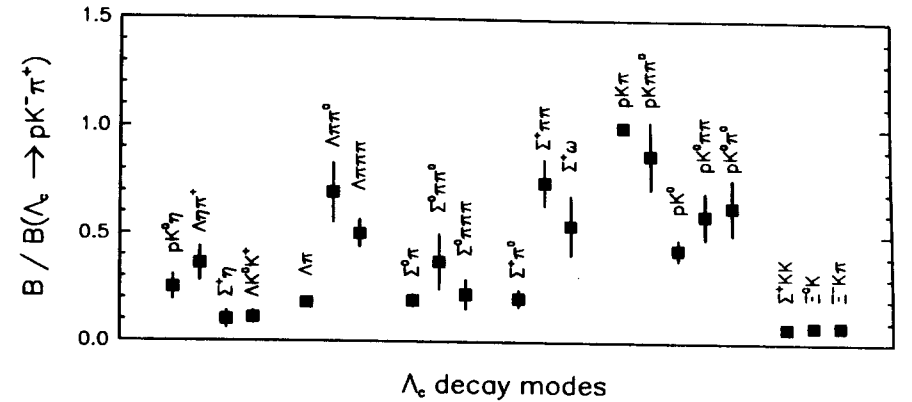


FIG. 1. Branching fractions of Λ_c^+ decays relative to the normalizing decay mode $\Lambda_c^+ \rightarrow pK^-\pi^+$ from recent CLEO measurements.

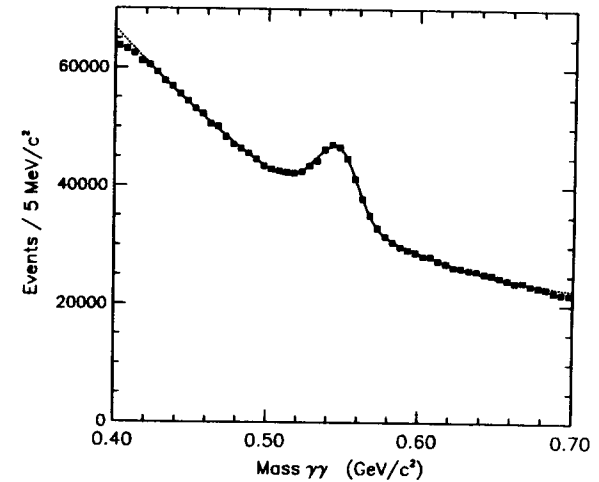


FIG. 2. Invariant mass distribution for $\eta \rightarrow \gamma\gamma$ with $P_\eta > 0.5$ GeV/ c .

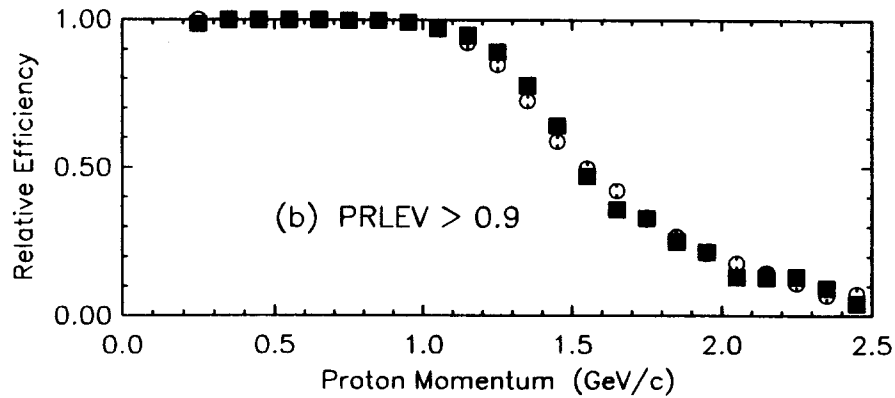
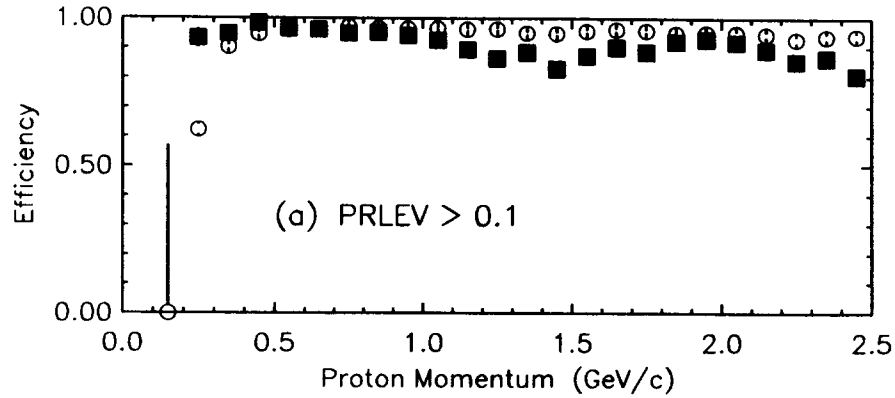


FIG. 3. Efficiency for selecting real protons with a weak or strong particle ID as a function of momentum for data (closed squares) and Monte Carlo (open circles). (a) PRLEV>0.1 efficiency, and (b) PRLEV>0.9 efficiency relative to the efficiency for protons to satisfy PRLEV>0.1.

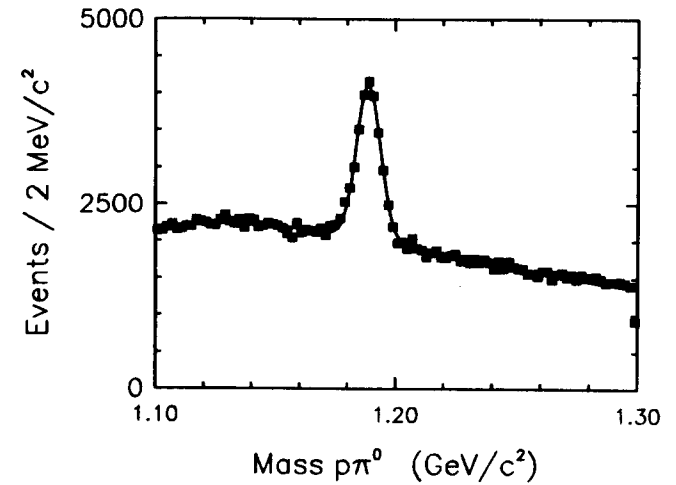


FIG. 4. Invariant mass distribution for $\Sigma^+ \rightarrow p\pi^0$ with $P_{\Sigma^+} > 1$ GeV/c.

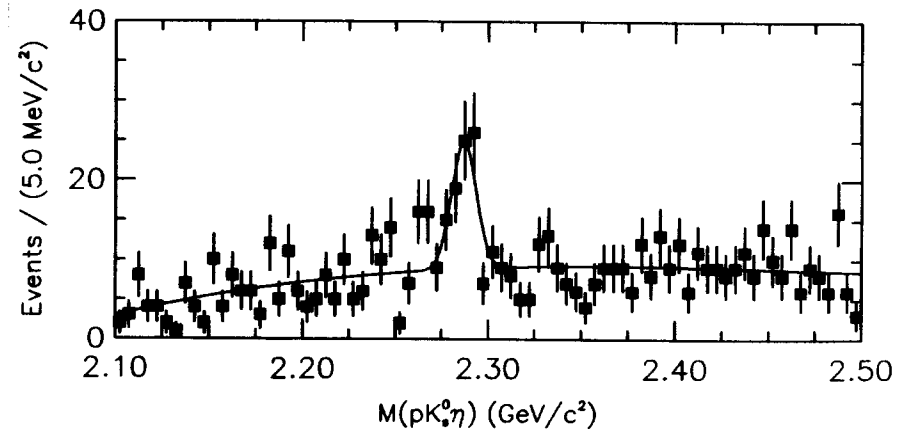


FIG. 5. Invariant mass distribution for $\Lambda_c^+ \rightarrow pK^0\eta$.

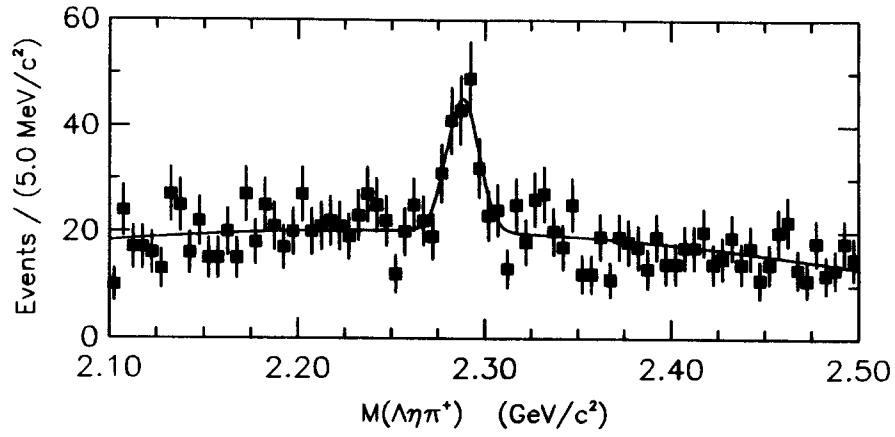


FIG. 6. Invariant mass distribution for $\Lambda_c^+ \rightarrow \Lambda \eta \pi^+$.

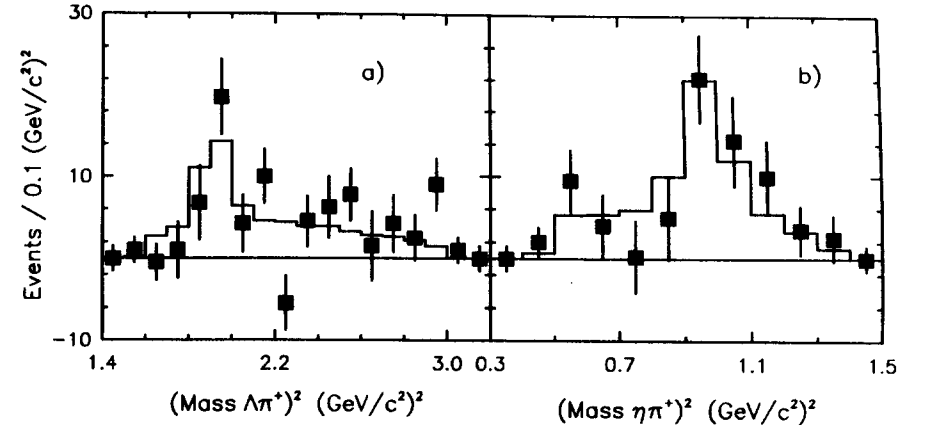


FIG. 8. Projection of Dalitz plot in the previous figure onto (a) the $M_{\Lambda \pi^+}^2$ axis and (b) the $M_{\eta \pi^+}^2$ axis

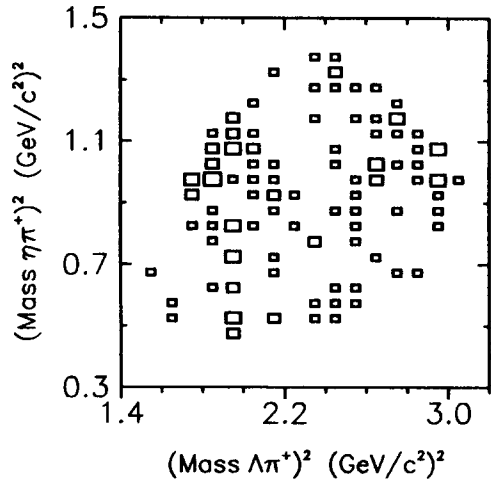


FIG. 7. Dalitz distribution for $\Lambda_c^+ \rightarrow \Lambda \eta \pi^+$: $M_{\Lambda \pi^+}^2$ versus $M_{\eta \pi^+}^2$

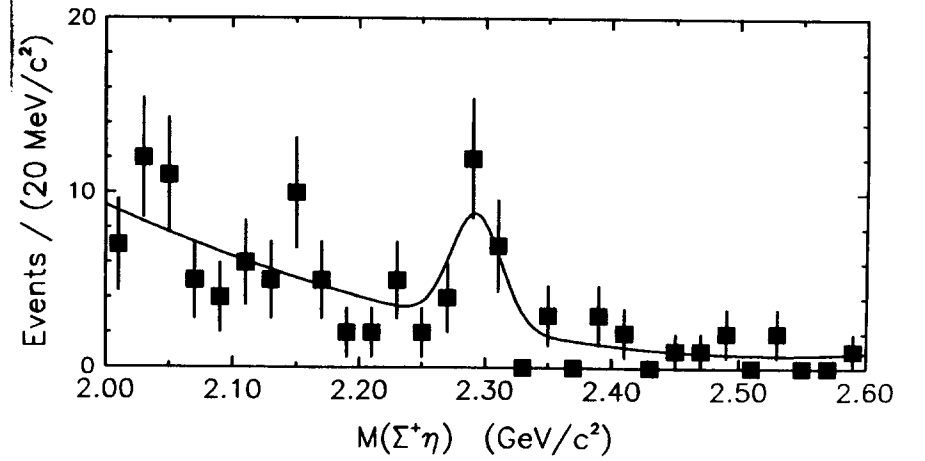


FIG. 9. Invariant mass distribution for $\Lambda_c^+ \rightarrow \Sigma^+ \eta$

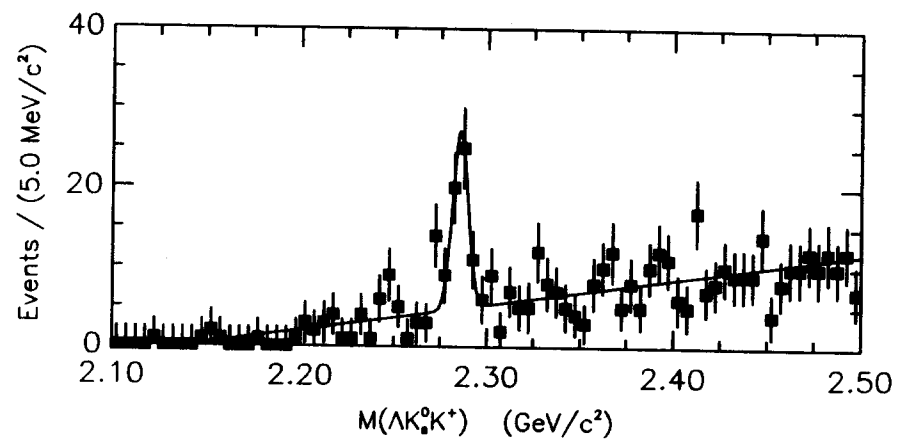


FIG. 10. Invariant mass distribution for $\Lambda_c^+ \rightarrow \Lambda K^0 K^+$

